THE PENNSYLVANIA STATE UNIVERSITY
SCHREYER HONORS COLLEGE

DEPARTMENTS OF ENERGY AND MINERAL ENGINEERING and ELECTRICAL ENGINEERING

IT'S ALWAYS SUNNY IN PHILADELPHIA: OPTIMIZING MULIT-SITE PV POWER OUTPUT VARIABLITIY IN EAGLEVILLE PA

GREGORY JAMES MOROZZI
SPRING 2013

A thesis
submitted in partial fulfillment
of the requirements
for a baccalaureate degree
in Electrical Engineering
with interdisciplinary honors in Electrical Engineering Energy and Mineral Engineering

Reviewed and approved* by the following:

Jeffrey R. Brownson
Assistant Professor of Energy and Mineral Engineering
Thesis Supervisor

Timothy J. Kane
Professor of Electrical Engineering and Meteorology
Honors Adviser

Mark S. Klima
Associate Head Energy & Mineral Engineering
Honors Advisor

* Signatures are on file in the Schreyer Honors College.

ABSTRACT

The variability of photovoltaic energy generation can be significant, and multiple studies have shown the relationship between space and time with respect to distributed PV generation. When multiple PV systems spread across a geographic region are connected to form an integrated network of distributed energy, the variability incurred on the electricity grid can be reduced in proportion to $\frac{1}{\sqrt{N}}$, where N is the number of systems. The main focus in many past studies has been on how more PV systems address the problem of variability, yet this is not necessarily always a valid method. This case study uses a network of irradiation sensors collecting data over ten days throughout Eagleville, PA to build a data set that will serve as a snapshot of what a reduced variability system could look like considering strategic numbering and placement of PV cells. By applying the method of Rayl, Young, and Brownson for calculating Power Spectral Density and Variance, measured values of uncertainty were calculated for 10 days, 1 day, and 1 hour intervals. [1] The results show that as the time interval of interest decreases in size, variance values decrease and from site to site the variances are on the same order of magnitude. The information gained from this experiment provides initial groundwork to evaluate how functioning PV systems would work in a decentralized power scenario. Information of this type could be useful to the Mid-Atlantic ISO through hour ahead and day ahead planning with regard to decentralized PV networks.

TABLE OF CONTENTS

LIST OF FIGURES

LIST OF TABLES

ACKNOWLEDGEMENTS

This thesis is a product of all the support and motivation provided by those around me. I wish to sincerely thank Dr. Jeffrey Brownson for accepting me into his research group and for his guidance throughout the process. His outlook on the research and writing process is something I valued during my time working with the group. Thank you to Dr. Timothy Kane who has showed his support throughout this process but also throughout the four years I have spent under his guidance in the Electrical Engineering department. Than you to Dr. Mark Klima who graciously served as my honors advisor in the College of Energy and Mineral Engineering. Special thanks to Lucas Whitmer whose help and guidance was instrumental in developing sound experiment and analysis techniques. Most importantly, I would like to thank James, Dorothy, and Matt Morozzi for emphasizing the importance of education and for their unending support in every aspect of life.

Chapter 1

Introduction

Regional transmission operators and power distributors are not in a position to implement solar energy into the grid efficiently because of the variability with which power is generated from sunlight at any given time. Still, is it recognized by Regional Transmission Operators (RTOs) and Independent System Operators (ISOs) country-wide that solar has huge potential to fill a key part of US power demands. This project aims to use co-spectrum analysis, meaning the analysis of irradiance at two or more generation points, to define the variance in power generation at a given time throughout the region of Eagleville Pennsylvania (40.1594° N, 75.4086° W). By understanding the volatility of solar power due to short term weather patterns in the Philadelphia region, this project will attempt to provide information to solutions that can maximize energy efficiency. More specifically, the project will target information that will be helpful to hour ahead and day ahead planning for RTOs and private companies wishing to bid for capacity.

Studies reported in "Irradiance co-spectrum analysis: Tools for decision support and technological planning" include spatial and temporal considerations for solar generation. [1] Certain conclusions from the study expand on the Taylor hypothesis that states the spatial averaging imposed by a solar array in the multi-megawatt range acts to damp variability in generation at high frequencies. "Integration of Renewable Generation in California" by Alexandra von Meier discusses the challenges associated with balancing instantaneous power in a network with multiple intermittent renewable sources of electricity. [2] Integrating under the curve of a Power Spectral Density graph, for multiple generation sources, statistical evidence can

be presented that will provide critical information to RTOs. Studying small intervals in this analysis will allow information to be collected on a minute by minute basis, therefore providing a starting point to use prediction of solar variability as a way to integrate solar generation into base load situations rather than using it simply to offset peaks in demand.

By taking relevant methodology and conclusions from “Irradiance co-spectrum analysis”, “Integration of Renewable Generation in California”, and multiple others sources and applying them to the Eagleville area, information gathered about the variability in the region will be a stepping stone for further research to build a plan for RTOs and private companies to implement next hour and next day generation techniques that optimize solar generation among different decentralized sources.

Chapter 2

Literature Review

Solar energy currently makes up a very small portion of the total power generated in the United States. Among other factors, intermittency plays a major role in keeping solar generation less efficient than desired, yet experts in the field agree that the research and development happening today gives solar generation significant potential to be a key player in global power production. Many studies today focus on understanding factors that cause intermittency and how it is possible to use this knowledge to maximize solar efficiency.

2.1 Co-Spectrum Analysis

The work of Rayl, Young and Brownson measures raw irradiance data and shows that it can be coupled across spatial and temporal coordinates so that variability, phase and coherence may be obtained as tools for solar analysis in a particular region. [1] This study uses Rayl, Young and Brownson's "Tools for decision support and technological planning" to analyze the Eagleville region.

The first area of interest is power spectral density (PSD), which is the distribution of a signal's variance across time scales. In Jenkins and Watts' work it's shown that Parceval's relation states the sum of power spectral density over all periodicities is equal to the variance of the original signal. [6] Since, variance over time scales is a key part of analysis for this project we use theory established in equation 2-1 to determine the variance contribution of our periodicities of interest.

(2-1)

$$var(x) = \frac{1}{T}\int_{\frac{-T}{2}}^{\frac{T}{2}} x^2(n)dn = \sum_{m=-\infty}^{\infty} |S_m|^2$$

Coherency and phase spectra are two components of the co-spectrum. Analysis of the co-spectrum arises when power spectral density is measured between two arrays of data. The coherency spectrum is an indicator of the correlation between the two arrays of data while the phase spectrum measures the lead or lag between the two signals as shown in equations 2-2 and 2-3 respectively. These measures can also be helpful in analyzing raw irradiance data for spatial averaging purposes.

(2-2)

$$K_{xy}(\omega) = \frac{\alpha_{xy}(\omega)}{S_{xx}(\omega)S_{yy}(\omega)}$$

(2-3)

$$\phi_{xy}(\omega) = tan^{-1}\left(\frac{Im\big(S_{xy}(\omega)\big)}{Re\big(S_{xy}(\omega)\big)}\right)$$

Results from Rayl, Young and Brownson depicted in table 2-1 show that, by collecting information in time and space, different variance values are recognized based on location and season. The authors later explain that information they collected can be helpful in addressing challenges like planning for day ahead markets, service and restoration power management time scales, and hour ahead markets. Specific results can be drawn about how to address these challenges by using figure 2-1 which is a figure developed by the authors intended to relate spatio-temporal scales to specific metrological phenomena.

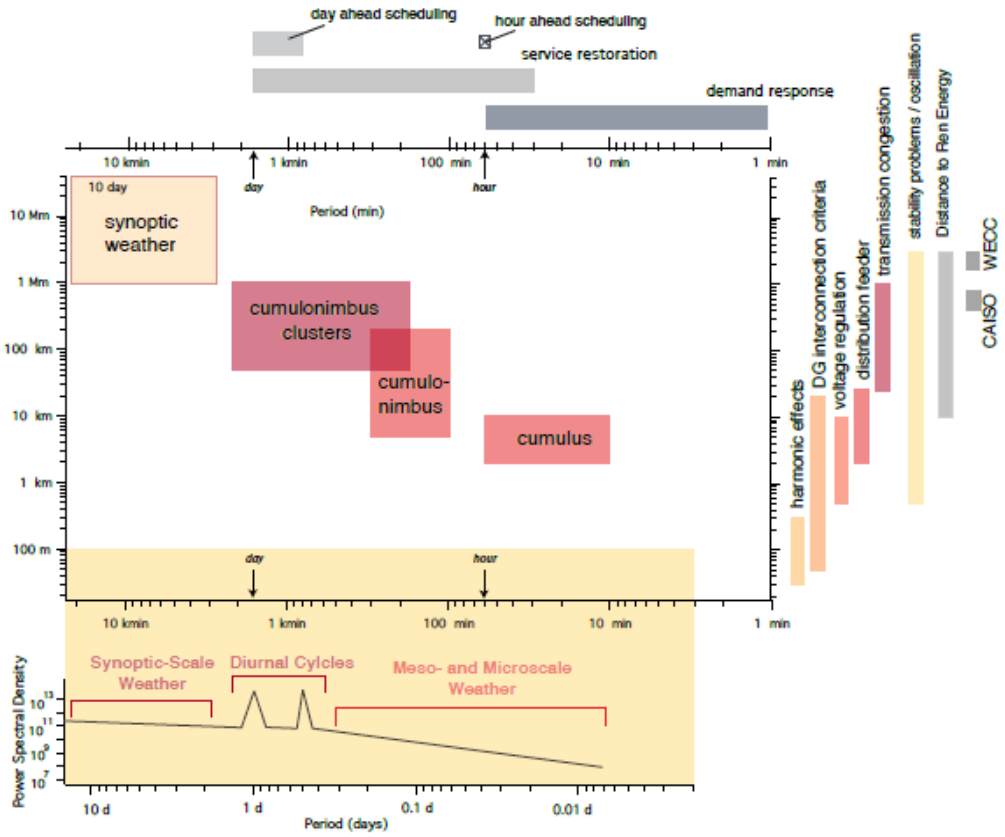

Figure 2-1. Graphic illustrating the scales of weather adapted from Fujita (1981) and diurnal phenomena on logarithmic scales of time and space. Complementary scales of power systems and meteorological power spectral density are also shown. Power Systems data from von Meier (2011).

Table 2-1. Quantitative variance for Sterling, VA and Rock Springs, PA in three select bands for each season and location

Season	Total:	STE	PSU
Win	(entire time series)	8.682 e 03	9.390 e 03
Spr		3.009 e 04	3.216 e 04
Sum		4.060 e 04	4.083 e 04
Fall		1.597 e 04	1.726 e 04
Season	Day ahead:	STE	PSU
Win	(0.5 day to 1 day):	2.644 e 03	1.699 e 03
Spr		1.057 e 04	0.972 e 04
Sum		1.480 e 04	1.444 e 04
Fall		5.472 e 03	4.920 e 03
Season	Service restoration:	STE	PSU
Win	(0.2 day to 1 day):	2.679 e 03	4.029 e 03
Spr		1.251 e 04	1.345 e 04
Sum		1.788 e 04	1.854 e 04
Fall		6.846 e 03	7.575 e 03
Season	Hour Ahead:	STE	PSU
Win		2.883 e -01	3.842 e -01
Spr		1.275 e 00	1.089 e 00
Sum		3.058 e 00	2.551 e 00
Fall		6.501 e -01	5.791 e -01

2.2 Station Pair Correlation and Variability

Studies related to the arrangement of PV fleets have been going on for quite some time. Most research agrees that as the number of sites (N) increases, the net effect on the system is that it will dampen variability proportional to $\frac{1}{\sqrt{N}}$, alternatively described by financial and investment analysts as the portfolio effect. Research recorded by Hoff and Perez takes this basic principle and adapts it to develop the dispersion factor; a new variable that captures the relationship between PV fleet configuration, cloud transit speed, and the time interval over which variability is evaluated (see equation 2-4). [3] The optimal point in solar generation is described as the point where the number of PV systems equals the dispersion factor meaning that a cloud disturbance

affecting one PV system will affect the next in exactly one time interval. An illustration of the optimal point is show in figure 2-2. After an extensive study of sixteen virtual networks throughout the United States, the results of the experiment imply that increasing the number of PV systems does not necessarily reduce the relative output variability within a crowded region such as a central generation plant. Hoff and Perez call for validation of this framework based on actual rather than virtual networks as is the case with the network we set up in Eagleville, PA.

$$D = \frac{L}{V\Delta t} \qquad (2\text{-}4)$$

*Where L = length of PV fleet in direction of cloud motion. V= transit rate and Δt = time interval

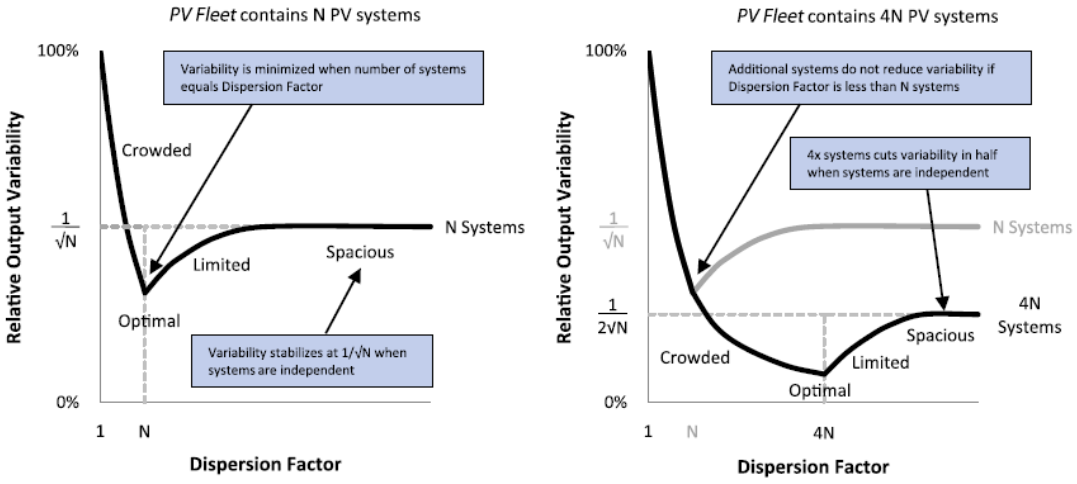

Figure 2-2. Relative Output Variability is a function of the number of PV systems and the Dispersion Factor.

Results from Perez Et al. show that distance between generation points play a significant role in damping variability. [4] Figure 2-3 displays the relationship between station correlation and station pair difference. As shown, the optimal point which is the lowest point on the curve, shifts depending on the sampling frequency. Studying these trends is important because the optimal

point shows where station pair is most uncorrelated, and therefore the point that is most valuable. In their experiment, the authors of this paper were able to determine ranges of optimal distance for discrete sampling frequencies. This principle is also shown in figure 2-4, which depicts the sampling frequency's effect on variability; namely that as the time interval increases, less opportunity for uncorrelated generation exists.

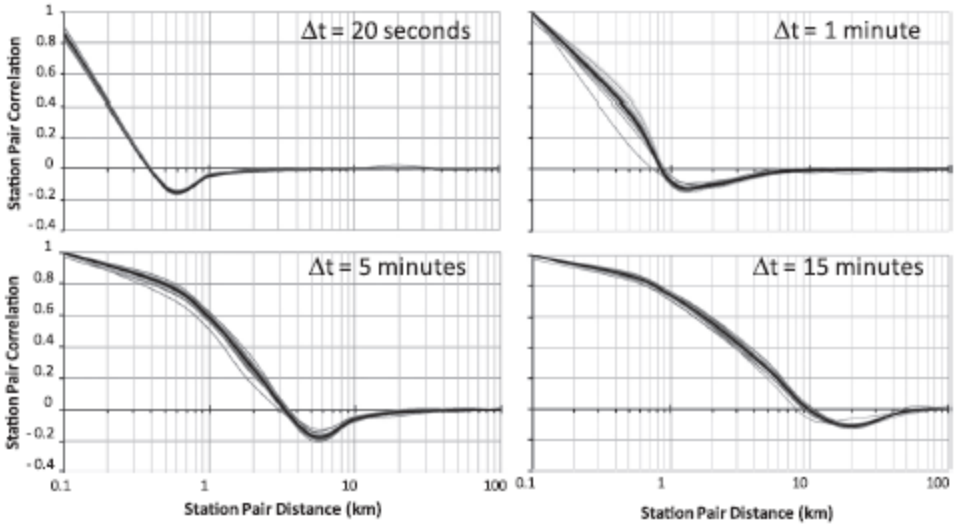

Figure 2-3. Single virtual network, single day station pair correlation as a function of distance and time scale.

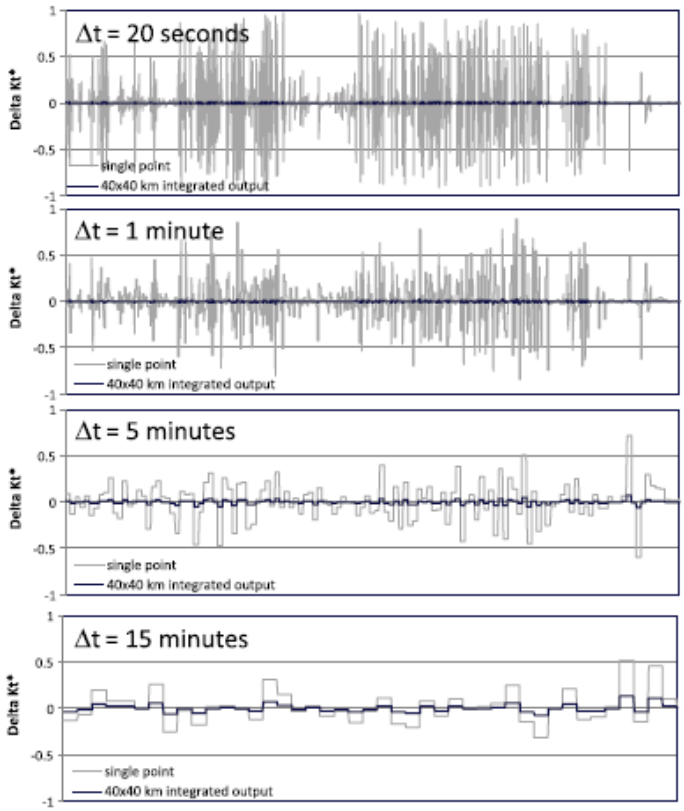

Figure 2-4. Comparing single site ad 40 x 40 km extended variability for different fluctuation time scales (at 20 s, the considered area includes ~64,000 uncorrelated locations and at 15min it includes ~ 16 such locations).

2.3 Solar Case Studies

Several case studies have been done with intent similar to this project; namely, to provide critical information about factors that enhance and impede efficient solar generation in a given area. After studying the current renewable generation platform in California, Alexandra von Meir states several factors that impede solar including: the time lag between California's solar generation peak and afternoon demand, solar output variation due to passing clouds on the order of minutes and seconds, and limited forecasting abilities especially on the order of minutes. [2] Her proposed solution to maximizing the efficiency of solar includes innovation in the areas of generation, storage, and demand response with a primary focus on time scales less than one hour.

Developing plans to maximize variance and coherence benefits through the sub-hour study of both meteorological and generation systems continue to appear as a common motif in the development of solar generation.

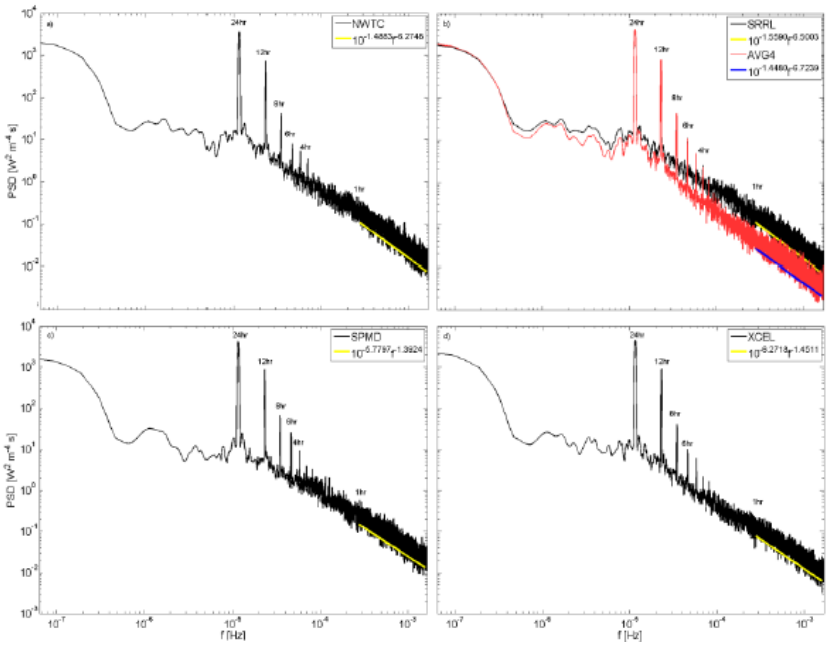

Figure 2-3. Power spectral density of (a) NWTC (b) SRRL and AVG4 (c) SPMD, and (d) XCEL for 2008 using 5 minute averaged GHI data.

In the work of Lave and Kleissl the authors performed a more hands on case study by studying variability at four different points across the state of Colorado. The study was done by analyzing variability in Global Horizontal Irradiance (GHI) rather than PV array power output, keeping in mind that important conclusions can still be drawn from GHI. [5] For example, the authors found that "a significant smoothing effect was observed when the averaged solar irradiance at four solar sites across Colorado is compared to the individual sites". Figure 2-7 depicts the Power Spectral Density plots for each of the four points. The PSD analysis shows a significant decrease in mean PSD at intervals shorter than one hour, therefore reaffirming the concept of reduced high frequency fluctuations in wind and solar distributed generation.

Chapter 3

Experimental Design and Setup

3.1 Data Collection

The data collected represents the irradiance readings for a portion of Eagleville PA, a suburb in the Philadelphia region. The readings are taken from four separate irradiance detectors called FireFlys, which were manually built for solar and temperature research at Carnegie Mellon University as seen in Figure 3-1. The sensors are programmed using a Visual Basic based language. The program is structured so that the amount of light incident on a sensor is measured and converted to a voltage value through a linear relationship every 20 seconds. The collected data is then written to an SD chip once every hour over the course of the two week experiment.

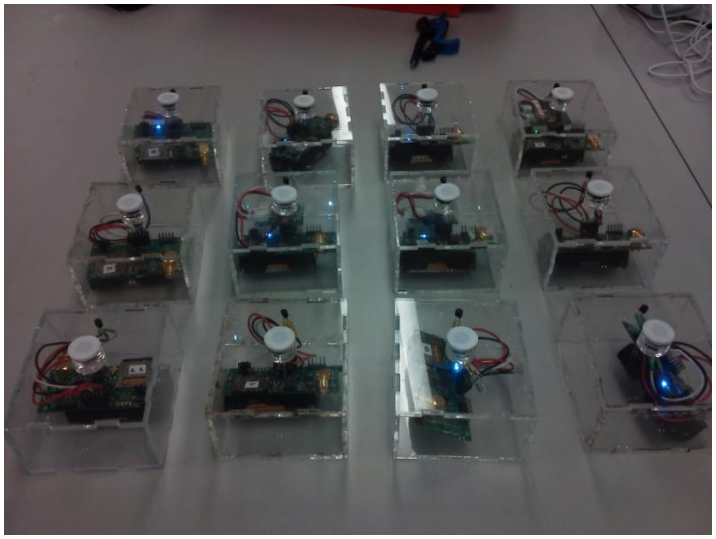

Figure 3-1. FireFly Capture

As explained by Hoff and Perez, the sampling frequency used when collecting irradiance data has an effect on the optimal distance between each node. [3] Specifically, for a sampling frequency of 20 seconds, the optimal distance between two nodes is in the range of .5km to 1km. Trying to keep this range in perspective while ensuring a reasonable and safe placement, the sensors recorded data at the given coordinates in table 3-1. A map of the four nodes, seen in Figure 3-2, is depicted to show the geometric shape of the intended collection points. The nodes were spaced out so that regardless of the direction of cloud speed, the nodes would not be in a straight line and thereby preserving the opportunity for spatial averaging.

Table 3-1. Sensor Locations

Node	Address	Lat./Long.
10	9003 Trolley Ln, Eagleville, PA 19403	40.1544, -75.3839
5	83 Egypt Rd, Eagleville, PA 19403	40.1329, -75.3830
8	Green Ridge Dr, Eagleville, PA 19403	40.1628, -75.3617

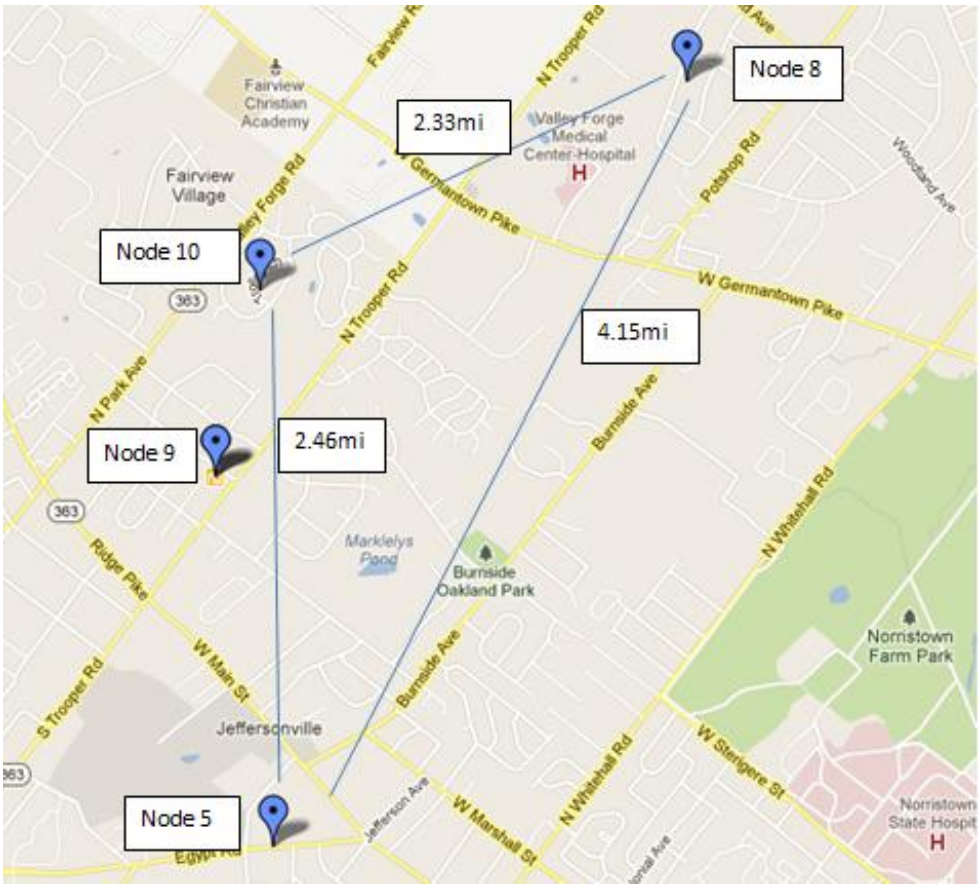

Figure 3-2. Sensor Map

3.2 Data Processing

All of the data collected from the test points in the Eagleville region was loaded into a spreadsheet and then time and magnitude adjusted. The data collected produced four arrays of voltage values (correlating directly to irradiance) over the course of fourteen days. To ensure that the start of each day was recognized by each of the sensors at exactly the same time, the four X axes (one for each array) were reconciled. In addition, to make the data more readable, the magnitude of node 5 was adjusted using a scalar factor function. These adjustments preserve the integrity of the raw data but help display it in a format so that it is easier to read.

Table 3-2. Battery Voltage

Node	Starting Voltage (V)	Final Voltage (V)
10	2.98	1.26
5	3.00	1.84
8	2.96	1.64
*note: all measurements were taken across both AA batteries		

Some non-ideal aspects of the data collected should also be noted. The experiment was set to run for a period of 14 days, but battery voltage only allowed for 10 days of data collection. Since the batteries experience losses that decline linearly, the irradiance data collected should be magnitude adjusted with respect to table 3-2. Other factors that add to non-ideal irradiance data include shading from surrounding objects and in two cases, snow that covered the sensor of the node. Additionally, the internal clock of each node did not keep exact time. While the sampling frequency was set to 20 seconds, the output revealed an interval closer to 22.3 seconds. In the case of node 9, the internal clock shifted so drastically that the data collected was deemed insignificant.

Chapter 4

Results

4.1 Data Acquisition and Processing

The first piece of code used, listed in Appendix A, is PsD.m, which is used as a function that calls two arrays of voltage values from the spreadsheet file mentioned above. The raw data is taken from the spreadsheet and converted from the time domain to the frequency domain through use of the Fast Fourier transform function, and then augmented by shifting zero frequency components to the center of the array. The reason that the transform into the frequency domain is necessary is to be able to draw conclusions from the data using Power Spectral Density and Coherence plots, which both include X axes in the frequency domain; in this case Hertz.

The next piece of code used to process the raw data is also found in Appendix A under CandP.m. This m file calls the function "PsD" from PsD.m, which has inputs: data1, data2, total and outputs: psd11, psd22, dcohere1, dphase1, coh1, var1, var2. By obtaining the relevant outputs, the program is able to plot figures of Power Spectral Density as well as Coherence and Phase for arrays 10 with respect to 5 (10-5), 10 with respect to 8 (10-8), and 8 with respect to 5 (8-5). By running three iterations, one for each combination of nodes, it is possible to look at coordination in both time and space and how it plays a role in solar generation in Eagleville PA.

4.2 Data

The time and magnitude adjusted voltage values in Figure 4-1 represent varying levels of irradiance at three of the four nodes. With a Y axis of voltage and an X axis of time, this plot indicates that general trends in irradiance values are common among nodes, but due to the spatial separation of the nodes, as implemented based off of the work of Hoff and Perez, key differences in irradiance values arise when studied at a small time interval. [3]

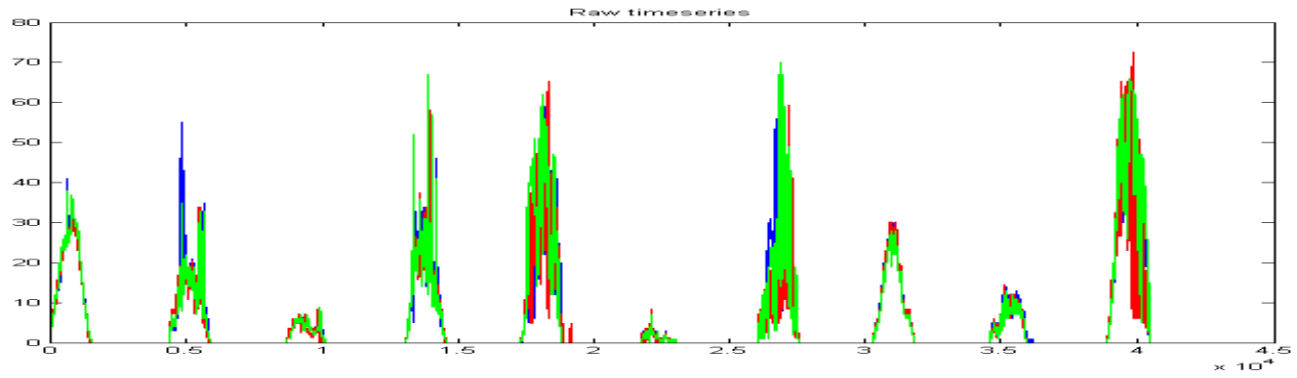

Figure 4-1. Raw time series Node10, 5, 8

As an example, day 5 is enlarged in Figure 4-2 to clearly show the discrepancies between values of Node 10, 5 and 8. While each node peaks around 60V, the max and min along with most other points on the curve occur at different times. With this result in mind we are able to see how coordination in time and space can lead to maximizing generation efficiency. For example, highlighting day 5 at the interval X: (1.849e-4: 1.861e-4), it can be seen that node 8 (green) almost mirrors node 10 (blue) across the line Y=26. This means that in a system implementing this arrangement of PV cells, the poor performance by node 10 during this short interval can be

leveraged by the excellent performance of node 5 during the same interval in which case the load recognizes little to no shift in input value.

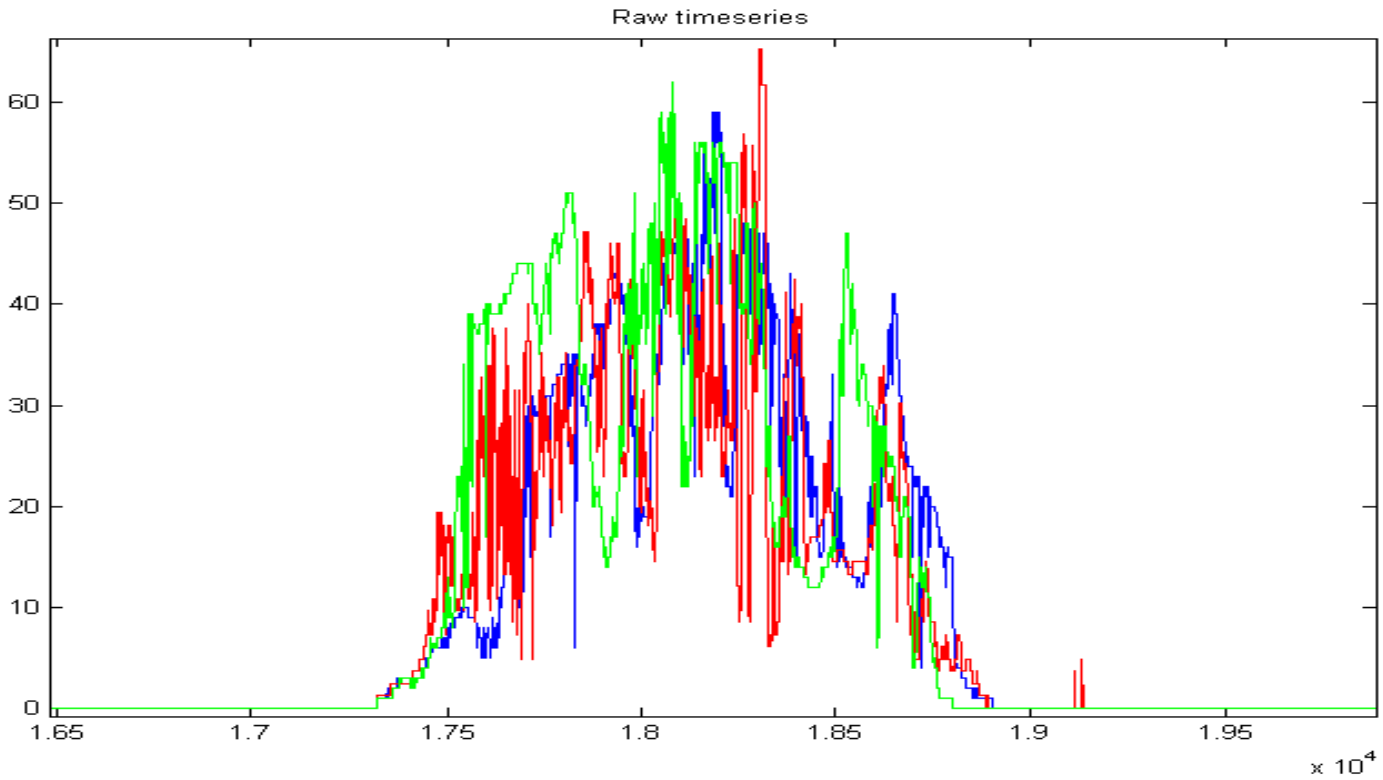

Figure 4-2. Timeseries Day 5

Table 4-1. Quantitative Variance for Node 10, 8, 5

	Node 5	Node 8	Node 10
Entire Time Series	32.16	46.83	43.78
Day Ahead	9.47	14.56	14.21
Hour Ahead	.85	.39	.26
*note: variance values calculated based off equation 2-1; (σ^2)			

As previously shown in the literature review section of this paper, power spectral density analysis is an important tool in studying the effects of coordination in time and space of a solar network. Figures 4-3, 4-4, and 4-5 show the PSD curves of nodes 10, 5 and 8 respectively where the X axis represents frequency [Hz] and the Y axis represents PSD [$W^2m^{-4}s$]. As expected, each curve displays diurnal peaks around 1 day and 12 hours with small phase differences between plots because of the short distance between nodes. It is important to note that for each of the three curves, both the left most region of the plot which represents diurnal cycle and the Meso- and Microscale which begins around X: (2e-4) have varying degrees of correlation. Delving into this correlation brings out the heart of variance analysis for purposes of day ahead and hour ahead scheduling.

By integrating under the curve of the PSD plot for certain periods of interest, we will gain the statistical variance for that period. Table 4-1 displays values for variances measured at each node with respect to special periods of interest. Since the aim of this project is to provide information that can be helpful to day ahead and hour ahead scheduling, the periods of interest are measured as follows. Day ahead forecasting aims to predict a full day's electric demand at the current half day. For this reason, the day ahead period of interest becomes 12 hours to 24 hours. Applying the same principle to hour ahead scheduling, the period of interest is .5 hours to 1 hour. The variance is also calculated over the period representing the entire time series for comparison (day 1-10). As seen in table 4-1, variance values are significantly bigger for 'Entire Time Series' (32-46) as compared to 'Day Ahead' (9-14). Also 'Day Ahead' values have a much bigger magnitude than those of 'Hour Ahead' (.25-.85).

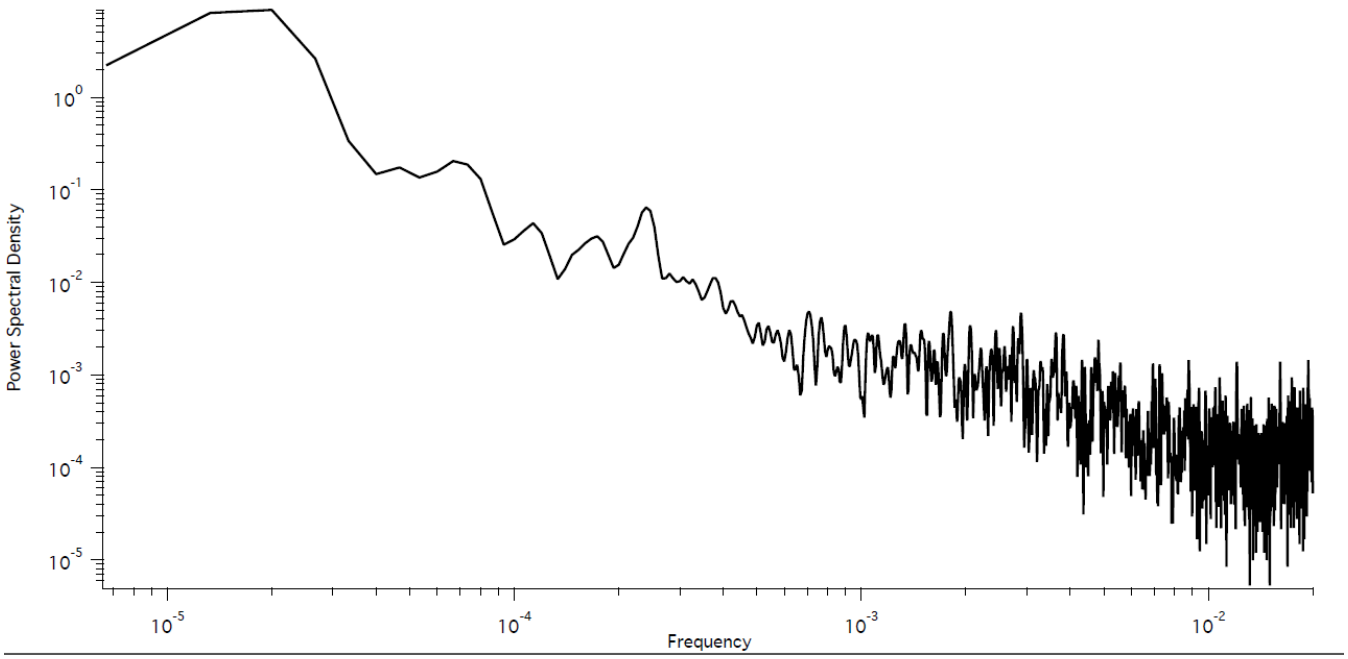

Figure 4-3. Power Spectral Density Node 10

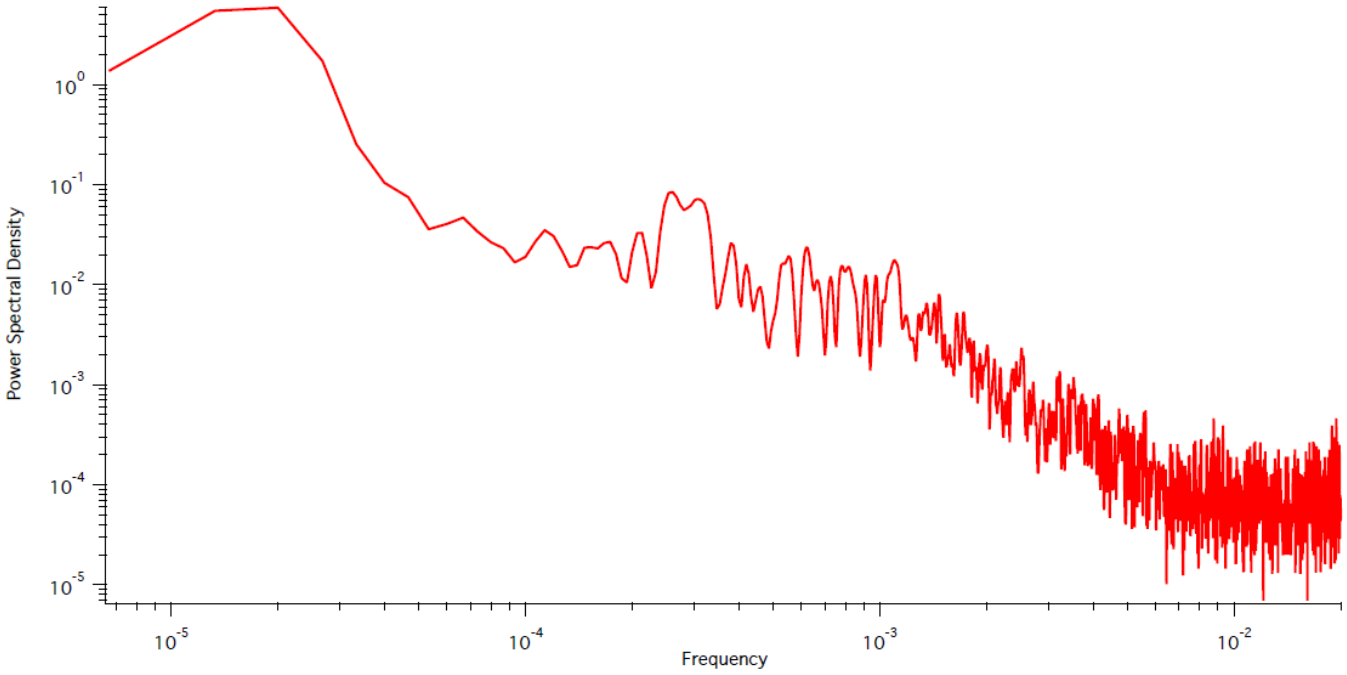

Figure 4-4. Power Spectral Density Node 5

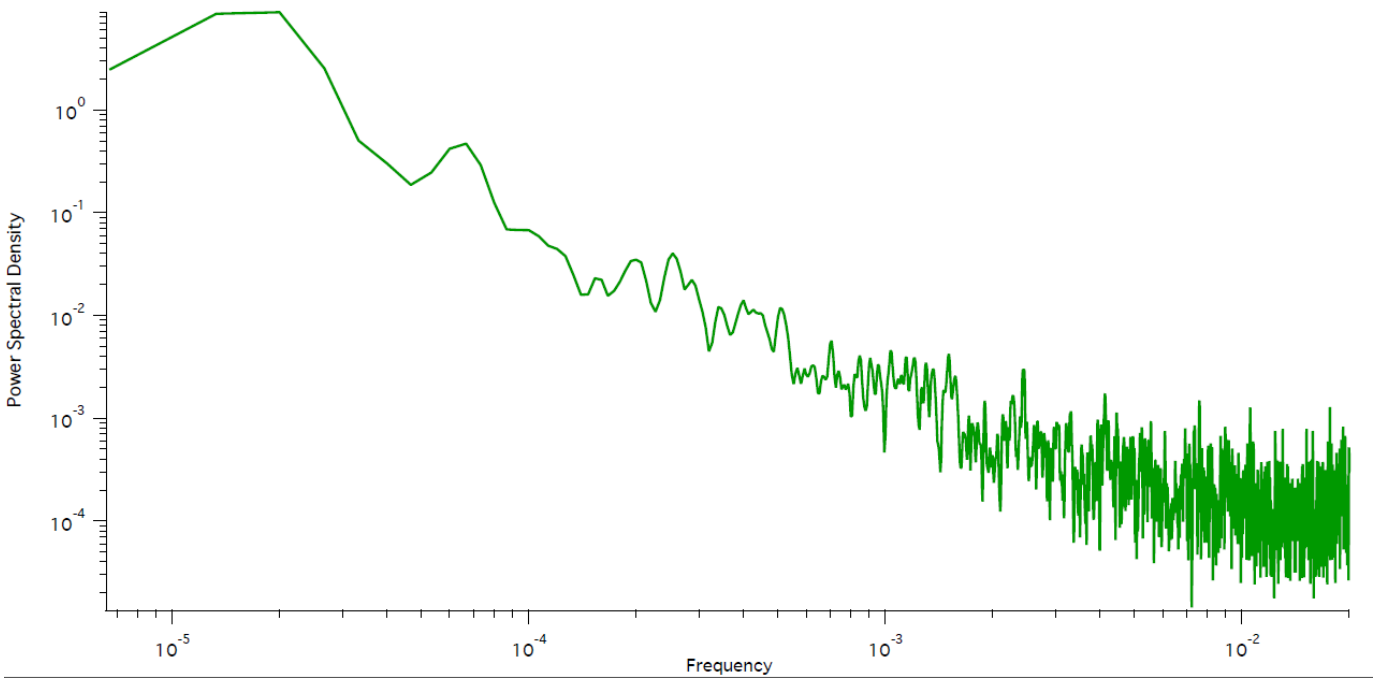

Figure 4-5. Power Spectral Density Node 8

4.3 Discussion

Central to the analysis of the data collected, are the variance values over a defined set of periodicities. Studying a node's variance is a way of measuring the amount of uncertainty contained at that nodes output. Looking at the data, this project shows that there exists a different statistical variance for each of the three nodes for the same region of defined frequency. From table 4-1 we see that as periodicities decrease in length, the amount of variance becomes smaller. This makes sense because over a full ten days, the amount of variability between nodes should be greater than that of an hour because there is a greater region for which each nodes irradiance data can deviate from each other.

The real value from this project comes from the fact that it is a simple and cost effective solution to collecting and studying irradiance in a region that proves to have variability at the diurnal and meso/micro scale. The fact that solar is growing very rapidly and has potential to represent a larger percentage of the grids generation needs means that studies like this one are very valuable to the Independent System Operators (ISO) and Regional Transmission Operators (RTO) nation-wide. With responsibilities to forecast day ahead and hour ahead markets, it is easy to see how ISOs and RTOs will rely heavily on studies that show the statistical variances of irradiance for arrays throughout a certain region. More specifically, as mentioned by von Meier, reliance on sub-hour data collection is an important focus point that will allow operators to better predict and respond to demand needs based off smaller variances produced by decentralized networks like the one studied in this project. [2]

Chapter 5

Conclusion and Future Work

Noting that, as timescales become smaller, variance values decrease is a clear indication that plans for next hour and next day generation must rely on frameworks from studies such as these to adapt and form effective generation techniques. After processing and analyzing the data collected in this project, table 5-1 shows the spread of the data. From the first to third quartile 75% of the data is represented, and shows that each set is on a similar order of magnitude.

Table 5-1. Table of Summary Statistics

	Min	1st Quartile	Median	Mean	3rd Quartile	Max
Entire Time Series	32.16	37.97	43.78	40.92	45.30	46.83
Day Ahead	9.47	11.84	14.21	12.75	14.39	14.56
Hour Ahead	.26	.33	.39	.50	.62	.85

Much like the call to action from Von Meier and Hoff and Perez, it is crucial that research and case studies of real PV networks continue. By nature the meteorological and geographic make-up of our nation is inherently varied. As such, specific plans based off empirical data collected in a particular region are critical to that region's successful implementation of renewable sources. Highlighting the Philadelphia area, the work laid out in this project only serves as a foundation. In order to develop a successful plan for next hour or next day generation based off of decentralized solar arrays, information on the power spectral density, variance, coherence, and phase must go deeper and wider. Deeper in the sense that more complex and accurate ways of measurement can be used to ensure precision in data collection, and wider in the sense that this

case study only represents a very small portion of the Eagleville area let alone the Philadelphia region.

In essence, this study has unlocked a key aspect of solar implementation that can be a huge asset to the Philadelphia region. The work suggests that meteorological information is central to combating problem of intermittency in generation. Even though it is not, in fact, always sunny in Philadelphia, research suggests that the future systems to be implemented in the region can make it seem as such.

Appendix A
Matlab Code

CandP.m

```
%Jeff Rayl
%Penn State EME Dept.
%Revised by Kyle Imhoff for Matlab from Scilab - May 29, 2012
%Program for calculating coherence and phase for several atmospheric
variables
%at one site.
%George Young edits as of 8/20/2012

%Greg Morozzi edits as of 3/13/2012

% Houskeeping
clear all
close all
clc
% Input data
A = xlsread('DecemberData_3_10_13.xlsx','A1:C42261');
size(A)
figure
plot(A(:,1))
hold on
plot(A(:,2),'red')
hold off
title('Raw timeseries')
data1 = A(:,1); %size of data array
data2 = A(:,2);
total=size(data1,1);

[psd11,psd12,dcohere1,dphase1,coh1,var1,var2] = PsD(data1,data2,total);


%  Check Parseval's relation
'var1 and var2'
[var1,var2];
[sum(psd11)/var1,sum(psd12)/var2] %output close to 1


figure
subplot(2,1,1)
loglog(psd11)
subplot(2,1,2)
loglog(psd12)
```

```
title('Power spectral plots')


figure
subplot(2,1,1)
plot(coh1, dcohere1)
ylabel('Coherence DWS vs Temp')
xlabel('Unfolded Frequency Bin (shifted)')
subplot(2,1,2)
plot(coh1,dphase1)
ylabel('Phase DWS vs Temp')
xlabel('Unfolded Frequency Bin (shifted)')


% Output
csvwrite('myOutputFile.csv',[psd11,psd12,dcohere1,dphase1,coh1])
```

PsD.m

```
%Jeff Rayl
%Penn State EME Dept.
%Revised by Kyle Imhoff for Matlab from Scilab - May 31, 2012
% 2nd Revision : code modified by JRSBrownson on Aug 20, 2012
%Function that calculates the coherence and phase for two input data
arrays.

%Greg Morozzi edits as of March 13, 2013

function [psd1, psd2, dcohere, dphase, coh, var1, var2] =
PsD(dataArray1,dataArray2,total) %declaration of the function
PSDCoherenceAndPhase

clear ap;
clear bp;
clear fap;
clear fbp;
clear cop;
clear qp;
clear gsyhan;
clear gsyhanCol;
clear fftpsd1;
clear fftpsd2;
clear psd1;
clear psd2;
clear dcohere;
clear lcohere;
clear coh;
clear dphase;
```

```
%  JRSB adding variance terms for the two spectra to be compared
clear var1;
clear var2;

m=10;
nw=total/m;
startpt=1;
endpt=nw;
gasum=zeros(nw,1); %creates array of all zeros
gbsum=zeros(nw,1);
psd1=zeros(nw,1);
psd2=zeros(nw,1);
gabsum=zeros(nw,1);
gsyhan=window(@hamming, nw);  %This is a George S Young convention
(gsy) and typo "hn" should have been "hm"
%window = designs an FIR filter using specs based on hamming
qsum=zeros(nw,1);
cosum=zeros(nw,1);
% JRSB adding variance zeros
var1=0;
var2=0;


gsyhanCol(:,1) = gsyhan; %applies the function to each element of the
array

for i=1:m
    ap=detrend(dataArray1(startpt:endpt,1)); %detrend simply removes
linear trends

    ap=ap.*gsyhanCol;
    bp=detrend(dataArray2(startpt:endpt,1));
    bp=bp.*gsyhanCol;
    % JRSB adding variance calculation for detrended data
    var1 = var1 + var(ap);
    var2 = var2+ var(bp);

    fap=fft(ap);
    fbp=fft(bp);
%     fftpsd1 = abs(fft(dataArray1(startpt:endpt,1))).^2;
%     fftpsd2 = abs(fft(dataArray2(startpt:endpt,1))).^2;
    fftpsd1 = abs(fft(ap)).^2; %fast fourier transform
    fftpsd2 = abs(fft(bp)).^2;
    fap=fftshift(fap); % shifts 0 frequency component to center of
array
    fbp=fftshift(fbp);
    cop=(real(fap).*real(fbp) + imag(fap).*imag(fbp));
    qp=(imag(fap).*real(fbp) - real(fap).*imag(fbp));

    gap=abs(fap).^2;
    gbp=abs(fbp).^2;

    gasum=gasum+gap;
```

```
    gbsum=gbsum+gbp;

    psd1 = psd1 + fftpsd1;
    psd2 = psd2 + fftpsd2;
    gabp=conj(fap).*fbp;
    gabsum=gabsum+gabp;
    qsum=qsum+qp;
    cosum=cosum+cop;

    startpt=startpt+nw;
    endpt=endpt+nw;

end


% JRSB adding m averaging for both psd1,psd2, and var1, var2
psd1 = psd1/(m*nw^2);
psd2 = psd2/(m*nw^2);
var1 = var1/m;
var2 = var2/m;


dcohere=(conj(gabsum).*gabsum)./(gasum.*gbsum);
lcohere = linspace(1,total/m,total/m);
coh(:,1)=lcohere;
dphase=atan(qsum./cosum);

end
```

Appendix B

Visual Basic FireFly Code

Main.c

```
/******************************************************************************
 *  Nano-RK, a real-time operating system for sensor networks.
 *  Copyright (C) 2007, Real-Time and Multimedia Lab, Carnegie Mellon University
 *  All rights reserved.
 *
 *  This is the Open Source Version of Nano-RK included as part of a Dual
 *  Licensing Model. If you are unsure which license to use please refer to:
 *  http://www.nanork.org/nano-RK/wiki/Licensing
 *
 *  This program is free software: you can redistribute it and/or modify
 *  it under the terms of the GNU General Public License as published by
 *  the Free Software Foundation, version 2.0 of the License.
 *
 *  This program is distributed in the hope that it will be useful,
 *  but WITHOUT ANY WARRANTY; without even the implied warranty of
 *  MERCHANTABILITY or FITNESS FOR A PARTICULAR PURPOSE.  See the
 *  GNU General Public License for more details.
 *
 *  You should have received a copy of the GNU General Public License
 *  along with this program.  If not, see <http://www.gnu.org/licenses/>.
 *
 *  Edited by Luke Whitmer and Greg Morozzi Dec 2012
 *
 ******************************************************************************/


#include <nrk.h>
#include <include.h>
#include <ulib.h>
#include <stdio.h>
#include <avr/sleep.h>
#include <hal.h>
#include <nrk_error.h>
#include <nrk_timer.h>
#include <nrk_driver_list.h>
#include <nrk_driver.h>
#include <adc_driver.h>
#include "mmc.h"


NRK_STK Stack1[NRK_APP_STACKSIZE];
nrk_task_type TaskOne;
void Task1(void);
```

```
NRK_STK Stack2[NRK_APP_STACKSIZE];
nrk_task_type TaskTwo;
void Task2 (void);
/*
  NRK_STK Stack3[NRK_APP_STACKSIZE];
  nrk_task_type TaskThree;
  void Task3 (void);
*//*
    NRK_STK Stack4[NRK_APP_STACKSIZE];
    nrk_task_type TaskFour;
    void Task4 (void);
  */
void nrk_create_taskset();
void nrk_register_drivers();
uint8_t kill_stack(uint8_t val);

// Don't put the MMC buffer in a task or it will go onto the stack!
uint8_t sectorbuffer[512];
uint8_t adcbuffer[512];
uint8_t prebuffer[512];
uint16_t adcpos;
uint32_t sector;
uint8_t transition = 0;
int
main ()
{
  //uint16_t div;
  sector = 0;

  nrk_setup_ports();
  nrk_setup_uart(UART_BAUDRATE_115K2);

  printf( "Starting up...\r\n" );

  nrk_init();

  nrk_led_clr(0);
  nrk_led_clr(1);
  nrk_led_clr(2);
  nrk_led_clr(3);

  nrk_time_set(0,0);
  nrk_register_drivers();
  nrk_create_taskset ();
  nrk_start();

  return 0;
}


void Task1()
{
  uint16_t cnt;
  int8_t val;
  uint8_t flagStore = 1;
```

```
printf( "Task1 PID=%d\r\n",nrk_get_pid());

cnt=0;
cardType = 0;
for (int i=0;i<10;i++)
  {
    val=mmc_init();
    if(!val) break;
  }

printf("mmc_init returns %d\n\r", val );
if(val)
  {
    if(val == 1) printf("SD card not detected..");
    if(val == 2) printf("Card Initialization failed..");

    nrk_led_set(RED_LED); // error in SD init
  }

switch (cardType)
  {
  case 1:printf("Standard Capacity Card (Ver 1.x) Detected!\n");
    break;
  case 2:printf("High Capacity Card Detected!\n");
    break;
  case 3:printf("Standard Capacity Card (Ver 2.x) Detected!\n");
    break;
  default:printf("Unknown SD Card Detected!\n");
    break;
  }

while(1) {
  if (flagStore == 180)
    {

     nrk_led_toggle(GREEN_LED);
     /*
       printf("READING!!!!!!\r\n");
       printf("sector %ld\n\r",sector);            // show sector number
       val=mmc_readsector(sector, sectorbuffer);    // read a data sector
       printf( "readsector returned %d\n\r",val );
       for(cnt=0; cnt<32; cnt++ )
       printf( "%d ",sectorbuffer[cnt] );
       printf("\n\r");
     */
     //printf( "ZERO !!!!!!!\r\n" );
     //val=mmc_writesector(sector, zerobuffer);    // write a data sector
     //printf( "writesector returned %d\n",val );
     if (transition){
       printf( "\rTRANSITION WRITING!!!!!!! %d\r\n",sector-1);
       val=mmc_writesector(sector-1, prebuffer);    // write a data sector
       printf( "writesector returned %d\n",val );
       transition = 0;
       for(cnt=0; cnt<adcpos; cnt++ )
         prebuffer[cnt] = adcbuffer[cnt];
```

```
        }
        printf( "\rWRITING!!!!!!! %d\r\n",sector);
        val=mmc_writesector(sector, adcbuffer);    // write a data sector
        printf( "writesector returned %d\n",val );
        if (val != 0){
          nrk_led_set(ORANGE_LED);
        }

        printf( "After write:\r\n" );
        val=mmc_readsector(sector,  sectorbuffer);     // read a data sector
        printf( "readsector returned %d\n",val );

        if(val==0)
          {
            for(cnt=0; cnt<32; cnt++ )
              printf( "%d ",sectorbuffer[cnt] );
            printf( "\n\r" );
          }
        //sector++;
        flagStore = 0;
       }
    flagStore++;
    nrk_wait_until_next_period();
  }
}

void Task2()
{
  uint16_t cnt=0;
  uint8_t fd,val,chan;
  uint16_t buf[3];
  adcpos = 0;
  float numfloat;

  printf( "Task2 PID=%d\r\n",nrk_get_pid());
  fd=nrk_open(ADC_DEV_MANAGER,READ);
  if(fd==NRK_ERROR) nrk_kprintf( PSTR("Failed to open ADC driver\r\n"));

  while(1) {
    nrk_led_toggle(BLUE_LED);

    if (adcpos > 511)
      {
       printf("OVERFLOW!!!!!!!!\r\n");
       cnt = 0;
       adcpos = 0;
       sector++;
       transition = 1;
      }

    chan = 1; // LIGHT
    val=nrk_set_status(fd,ADC_CHAN,chan); // Set ADC channel
    if(val==NRK_ERROR) nrk_kprintf( PSTR("Failed to set ADC status\r\n" ));
    val=nrk_read(fd,&buf[chan],2);        // Read ADC channel
    if(val==NRK_ERROR) nrk_kprintf( PSTR("Failed to read ADC\r\n" ));
    numfloat = buf[chan];
```

```
    adcbuffer[adcpos++] =
((uint8_t)(numfloat/2));//(uint8_t)(buf[chan]/10);//0.04>>8;   // Store in
adcbuffer
    printf( "\rchan:%d=%d pos:=%d\n",chan,adcbuffer[adcpos-1],adcpos-1); // PRINT
ADC

    chan = 4; // TEMP
    val=nrk_set_status(fd,ADC_CHAN,chan); // Set ADC channel
    if(val==NRK_ERROR) nrk_kprintf( PSTR("Failed to set ADC status\r\n" ));
    val=nrk_read(fd,&buf[chan],2);        // Read ADC channel
    if(val==NRK_ERROR) nrk_kprintf( PSTR("Failed to read ADC\r\n" ));
    numfloat = buf[chan];

    adcbuffer[adcpos++] = ((uint8_t)(numfloat-
150));//(uint8_t)(buf[chan]/10);//0.04>>8;   // Store in adcbuffer
    printf( "\rchan:%d=%d pos:=%d\n",chan,adcbuffer[adcpos-1],adcpos-1); // PRINT
ADC

    if (transition == 0){
      prebuffer[adcpos-1] = adcbuffer[adcpos-1];
      prebuffer[adcpos-2] = adcbuffer[adcpos-2];
    }
    nrk_wait_until_next_period();
  }
}


void
nrk_create_taskset()
{

// MMC
  nrk_task_set_entry_function( &TaskOne, Task1);
  nrk_task_set_stk( &TaskOne, Stack1, NRK_APP_STACKSIZE);
  TaskOne.prio = 1;
  TaskOne.FirstActivation = TRUE;
  TaskOne.Type = BASIC_TASK;
  TaskOne.SchType = PREEMPTIVE;
  TaskOne.period.secs = 20;
  TaskOne.period.nano_secs =0*NANOS_PER_MS;
  TaskOne.cpu_reserve.secs = 20;
  TaskOne.cpu_reserve.nano_secs = 0*NANOS_PER_MS;
  TaskOne.offset.secs = 0;
  TaskOne.offset.nano_secs= 0;
  nrk_activate_task (&TaskOne);
// ADC
  nrk_task_set_entry_function( &TaskTwo, Task2);
  nrk_task_set_stk( &TaskTwo, Stack2, NRK_APP_STACKSIZE);
  TaskTwo.prio = 2;
  TaskTwo.FirstActivation = TRUE;
  TaskTwo.Type = BASIC_TASK;
  TaskTwo.SchType = PREEMPTIVE;
  TaskTwo.period.secs = 20;
  TaskTwo.period.nano_secs = 0*NANOS_PER_MS;
  TaskTwo.cpu_reserve.secs = 20;
```

```
  TaskTwo.cpu_reserve.nano_secs = 0*NANOS_PER_MS;
  TaskTwo.offset.secs = 0;
  TaskTwo.offset.nano_secs= 0;
  nrk_activate_task (&TaskTwo);
}


uint8_t kill_stack(uint8_t val)
{
  char bad_memory[10];
  uint8_t i;
  for(i=0; i<10; i++ ) bad_memory[i]=i;
  for(i=0; i<10; i++ ) printf( "%d ", bad_memory[i]);
  printf( "Die Stack %d\r\n",val );
  if(val>1) kill_stack(val-1);
  return 0;
}

void nrk_register_drivers()
{
  int8_t val;

  // Register the ADC device driver
  // Make sure to add:
  //     #define NRK_MAX_DRIVER_CNT
  //     in nrk_cfg.h
  // Make sure to add:
  //     SRC +=
$(ROOT_DIR)/src/drivers/platform/$(PLATFORM_TYPE)/source/adc_driver.c
  //     in makefile
  val=nrk_register_driver( &dev_manager_adc,ADC_DEV_MANAGER);
  if(val==NRK_ERROR) nrk_kprintf( PSTR("Failed to load my ADC driver\r\n") );

}
```

Chapter 6 Bibliography

1] Y. B. Rayl, "Irradiance co-spectrum analysis: Tools for decsision support and technilogical planning," *Solar Energy,* 4 February 2013.

2] A. Von Meier, "Integration of renewable generation in California: Coordination challenges in time and space," in *11th International Conference on Electricity Power Quality and Utilization* , IEEE: Industry Applications Society and Industrial Electronics Society, Lisbon, Portugal, 2011.

3] T. E. Hoff and R. Perez, "Quantifying ov power output variability," *Solar Energy* , vol. 84, pp. 1782-1793, 2010.

4] R. Perez, S. Kivalov, J. Schlemmer, K. Hemker and T. E. Hoff, "Short term irradiance variability: Preliminary estimation of station pair correlation as a function of distance," *Solar Energy,* vol. 86, pp. 2170-2176, 2012.

5] M. Lave and J. Kleissl, "Solar variablity of four sites across the state of Colorado," *Renewable Energy* , vol. 35, pp. 2867-2873, 2010.

6] M. Taylor and G. Watts, "Spectral Analysis and it's applications," Holden-Day Inc., 1968.

ACADEMIC VITA

Gregory James Morozzi

Gjm5112@psu.edu

Education

B.S., Electrical Engineering, 2013, The Pennsylvania State University, State College, Pennsylvania

Honors and Awards

- Best Engineered Design Award – Engineering Design 100 competition sponsored by Shell Co.

Professional Experience

Motorola Mobility LLC; Home Division
Horsham, PA
Broadband Access Networks Product Management Intern
May 2012-April 2013

- Designed a moisture sensor circuit to improve the lifespan of Motorola's optical nodes and amplifiers in areas of high humidity and rainfall worldwide
- Improved the product recall process by creating a detailed technical document to aid cable operators in replacing RF amplifier parts throughout Latin America.
- Coordinated the initial stages of a redesign for an Optical Headend Control Module by collaboratively defining the technical and marketing requirements with engineering and management teams

PJM Interconnection; Contracted through Yoh Services, LLC
Valley Forge, PA
Interconnection Projects Intern
May 2011-August 2011

- Analyzed the mapping and documentation system for the high voltage transmission grid covering 13 states and the District of Columbia as part of a three member team
- Collaborated on a weekly basis with members contracted from Integral GIS Inc. to identify glitches and errors in programs built for PJM